U. S. ARMY
TRANSPORTATION RESEARCH COMMAND
FORT EUSTIS, VIRGINIA

TRECOM TECHNICAL REPORT 63-60

VISCOUS AND FORWARD SPEED EFFECTS ON UNBALANCED JETS IN GROUND PROXIMITY

Task 1D021701A04804
(Formerly Task 9R99-01-005-04)
Contract DA 44-177-TC-845

October 1963

prepared by:

HYDRONAUTICS, Incorporated
Laurel, Maryland

5328-63

HEADQUARTERS
U S ARMY TRANSPORTATION RESEARCH COMMAND
FORT EUSTIS, VIRGINIA

This is an interim report on a theoretical investigation of the flow of air jets in ground proximity. A previous report presented a theory which included the effects of viscosity on a two-dimensional wall jet. The theory was found to be adequate for the hovering mode. This report extends the theory to include the cases of forward velocity and small angular displacements in hover.

The theory indicates that the vortices or vortex-type flow induced by the viscosity of the air jets is of some importance to the stability of the annular jet Ground Effect Machine. The investigation is continuing with experiments to confirm the assumed vortical flow pattern.

WILLIAM D. HINSHAW
Project Engineer

WILLIAM E. SICKLES
Group Leader
Ground Effect Research Group

APPROVED.

FOR THE COMMANDER:

for LARRY M. HEWIN
Technical Director

Task 1D021701A04804
(Formerly Task 9R99-01-005-04)
Contract DA 44-177-TC-845
TRECOM Technical Report 63-60
October 1963

VISCOUS AND FORWARD SPEED EFFECTS ON UNBALANCED JETS IN GROUND PROXIMITY

Technical Report 241-2

Second of a Series of Reports Pertaining to the Theoretical Investigation of Air Jet Flow Fields in Ground Proximity

Prepared by
HYDRONAUTICS, Incorporated
Laurel, Maryland

for
U. S. ARMY TRANSPORTATION RESEARCH COMMAND
FORT EUSTIS, VIRGINIA

PREFACE

The work reported herein was conducted at HYDRONAUTICS, Incorporated under U. S. Army Transportation Research Command Contract Number DA 44-177-TC-845. The work was carried out and the report written by Mr. C. C. Hsu. The technical administrative representative of the U. S. Army Transportation Research Command for this project was Mr. William D. Hinshaw.

CONTENTS

ILLUSTRATIONS

SYMBOLS

A	augmentation factor
a	ratio of mean jet velocity and outward velocity
b	ratio of mean velocities of inward and outward mass flow
C_μ	thrust coefficient
f	entrainment function
g	a function depending on induced velocity in the vortex region
H	nozzle base height above ground
h	step height
J	jet momentum per unit length of nozzle slot
J_R	rear edge jet momentum per unit length
L	lift
ℓ	distance from step to separation
M_α	induced moment due to tilt angle
M_j	induced moment due to jet reactions
M_{vortex}	induced moment due to vortex flow
p	ambient pressure
p_b	base pressure
Δp	pressure difference in dead-air region
Δp_b	average base pressure distribution
$\Delta p_{b)vortex}$	induced pressure loss due to vortex flow
q_m	jet mass flow
R	radius of curvature of jet curtain

S	planform area of the nozzle base plate
s_c	distance along the jet path from the nozzle exit
t	nozzle thickness
U_e	nozzle exit velocity
$U_{e,R}$	rear nozzle exit velocity
U_o	uniform forward speed
$\bar{u}$	average velocity of the jet before impingement
$\bar{u}_u, \bar{u}_d$	average velocities of the inward and outward mass flow respectively
$\bar{u}_{ave}$	average induced velocity in the vortex region
W	half width of the nozzle base plate
α	tilt angle
γ	a constant, depending on the local shearing stress
ρ	density of the air
φ_o	divergence angle of the jet
φ_c	impingement angle of the jet

SUMMARY

A theoretical investigation of the two-dimensional ground effect machine in unbalanced operation and forward motion has been carried out. Although the assumptions and approximations involved in the present analysis are quite broad, the analysis has permitted a better understanding of the nature of the flow, particularly with regard to the influence of viscous effects.

IN UNBALANCED OPERATION

For small disturbances, the mean flow pattern under the machine is similar to that in the hovering condition. The formation of two counter-rotating vortices under the machine is the sole cause for inducing static instability. For large disturbances, the air jet in the low side becomes overfed, resulting in a cross flow under the machine. The overall effect of the cross flow is, in general, destabilizing. A typical numerical example is shown to give quantitatively the effect of tilt angles on augmentation factor and induced moment. A static stability derivative curve which shows a higher stability boundary than that which results from inviscid calculations is also given.

IN FORWARD MOTION

Two distinct flow regimes may appear, depending on whether the leading-edge air jet escapes upstream or goes under the machine. In the first case, one again finds essentially the characteristics of the flow observed under hovering conditions (ground cushion flow regime). In the second case, the flow resembles that of the jet-wing type. The jet flow fields in the ground cushion flow regime have been discussed in detail. Due to the pressure difference between the leading and trailing edges, a difference in jet momentum, in the direction of thrust, may be induced. As a consequence, a nose-down moment is also induced. The induced nose-down moments are diminished or intensified by the effect of the moving ground, depending on specific flow conditions. Typical numerical examples have also been made. It is found that at relatively low forward speeds, a considerable amount of thrust and nose-down moment may result.

CONCLUSIONS

A two-dimensional study can not pretend to provide an entirely accurate picture of the real ground effect machine in forward motion. However, even though the assumptions and approximations involved in the analysis presented are quite broad, it has permitted a better understanding than previously available of the nature of the flow associated with unbalanced operation and forward motion, particularly with respect to the influence of viscous effects.

IN UNBALANCED HOVERING OPERATION

For small disturbances, the formation of two major counter-rotating vortices under a hovering machine is the sole cause for inducing a moment. The induced moments were found to be stabilizing for $H/t < 5.2$ and destabilizing for $H/t > 5.2$.

For large distrubances, the edge jet on the low side becomes overfed. The cross flow due to the viscous action of the fluid may have dual effects on the static stability of the ground effect machine:

a) A stabilizing influence due to a friction effect.

b) A destabilizing effect due to diffusion.

For practical heights, the diffusion effect always outweighs the friction effect. The overall effect of the cross flow, in general, is thus destabilizing.

IN FORWARD MOTION

For a moving ground effect machine, two distinct flow regimes may appear:

a) Ground cushion flow regime - At relatively low forward speeds, the leading edge jet escapes upstream, and the characteristics of the flow are essentially the same as in the hovering condition.

b) Jet-wing type of flow regime - At high forward speeds, the leading edge jet deflects inward before reaching the ground, and the flow resembles that of the jet-wing type.

In the ground cushion flow regime, a difference in jet momentum, in the direction of thrust, may be induced due to the pressure difference between the trailing and leading edges. As a consequence, a nose-down moment is induced. This induced moment may be diminished or intensified, depending on whether the stronger vortex exists at the trailing or leading edge.

INTRODUCTION

In practice, there are three important aspects of ground effect machine design: hovering performance, maneuverability, and cruising performance. The effects of viscosity on the jet flow fields of a ground effect machine in the hovering condition have been studied in detail in an earlier report (1). The mean flow pattern is seen to be that of a diffusing jet which is deflected laterally in its interaction with the central pressure zone. When the ground effect machine is in unbalanced operation or in forward motion, the major characteristics of the jet flow fields in ground proximity, such as turbulent mixing and vortex generation, are similar to those for balanced jets in ground proximity. However, they are made somewhat more complicated because of the asymmetry and external flow conditions. The object of this report is to discuss, both qualitatively and quantitatively, some important effects on the behavior of the jet flow field which are due to unbalanced operation and forward motion of the ground effect machine.

It is very difficult to solve for the details of jet flow fields associated with an annular unbalanced jet in ground proximity. Fortunately, for small disturbances, simple and plausible approximations such as are used for balanced jets (1) may be made. The calculations on the effect of jet mixing are based on the entrainment process and momentum balance considerations in the impingement region. As to the effect of the standing vortex, the problem is reduced to that of calculating the inviscid rotational flow pattern in a closed region with uniform but undetermined vorticity, and the associated indeterminacy of the inviscid motion may be resolved by a simple analysis of the closed frictional boundary layer. At relatively low forward speeds, i.e., in the ground cushion flow regime, the jet flow fields under the machine may be calculated approximately in the same way. However, the jet flow field in the neighborhood of the leading edge is significantly different from that in the hovering condition due to the action of the oncoming stream. The resultant flow pattern in the region resembles somewhat the flow up a step and may be solved by a free streamline analysis.

EFFECT OF UNBALANCED OPERATION

We shall first discuss the jet flow fields of the ground effect machine in the maneuvering condition; that is, in unbalanced operation. When the ground effect machine is tilted, or when it is undergoing heaving motion, it is conceivable that, due to pressure differences under the edges of the machine, both underfed and overfed jet configurations, as first studied by Tulin (2), may exist. Although the major characteristics of jet flows in ground proximity, such as turbulent mixing and vortex generation, are similar to those of balanced jets as discussed in (1), they are made more complicated because of the overfed jet flow condition. The overfed jet, after impinging on the ground, splits into two parts: one flows outward to the ambient region, and the other flows inward and eventually merges with the other edge jet. The jet flow along the ground behaves like the turbulent "wall-jet" which has been studied theoretically by Glauert (3) and experimentally by Bakke (4) and Schwarz and Cosart (5). The "wall-jet" is of the self-preserving class of shear flows. In the outer layer, the flow has jet-like properties, while in the inner layer the flow is similar to that of the wall boundary layer. Because of the diffusing action of the inward flowing turbulent wall-jet stream, the flow field under the base plate can no longer be considered as stagnant. Unlike the case of balanced operation, in which one need only take account of the effect of the first major vortex standing alongside the edge jet, the characteristics of the annular jet in unbalanced operation cannot be completely determined without solving simultaneously for the combined flow composed of the induced rotational flow and the complete boundary layer (partly along solid surfaces and partly as jets). As an illustration, the jet flow field of a slightly tilted ground effect is studied in detail.

For a first-order analysis, the tilt angle, α, is assumed to be very small so that the flow pattern has not deviated very much from that in balanced operation (see Figure 1). It is then reasonable to assume that the basic assumption concerning jet impingement and jet mixing are, more or less, the same as that for balanced jets. The base pressure, Δp_b, across the jet due to jet mixing may be shown to be

$$\frac{\Delta p_{b,1}}{J_1/W} = \frac{\sin \varphi_{c,1} - \sin \varphi_{o,1}}{H_1/W} + \lambda_1 f \left(\frac{s_{c,1}}{t}\right)$$

$$\frac{\Delta p_{b,1}}{J_2/W} = \frac{\sin \varphi_{c,2} - \sin \varphi_{o,2}}{H_2/W} + \lambda_2 f \left(\frac{s_{c,2}}{t}\right) \qquad [1]$$

where

f is the entrainment function

J is the jet momentum per unit length

H is the nozzle height above the ground

s_c is the distance along the jet path

t is the nozzle thickness

W is the half width of the nozzle base

φ_o is the nozzle divergence angle

φ_c is the jet impingement angle

λ is a constant $\leq \frac{1}{2}$

and the subscripts "1" and "2" denote the quantities at the "low" and "high" sides of the ground effect machine respectively. The base pressure, without including the effect of standing vortices, is likely to be uniform; and its magnitude is seen to be limited to $\Delta p_{b,2}$, which is the pressure drop that the most vulnerable part of the jet, i.e., the part of the jet originating at the highest point of the nozzle, is capable of sustaining. It is apparent, from Equation [1], that if the jets are of equal strength and divergence angle, the impingement angle on the "low" side, $\varphi_{c,1}$, is, in general, less than that for the high side, or

$$\sin\varphi_{c,1} = \frac{H_1}{H_2}\sin\varphi_{c,2} + \left(1 - \frac{H_1}{H_2}\right)\sin\varphi_o$$

$$+ \frac{H_1}{W}\left[\lambda_2 f\left(\frac{s_{c,2}}{t}\right) - \lambda_1 f\left(\frac{s_{c,1}}{t}\right)\right] < \sin\varphi_{c,2} \, , \qquad [2]$$

since

$$\frac{H_1}{H_2} = \frac{H - W\sin\alpha}{H + W\sin\alpha} < 1$$

φ_o is generally inclined inward for better augmentation, that is, ≤ 0 ,

and

$$\frac{H_1}{W}\left[\lambda_2 f\left(\frac{s_{c,2}}{t}\right) - \lambda_1 f\left(\frac{s_{c,1}}{t}\right)\right] << 1 \text{ in ground proximity.}$$

The entrainment from the base cavity into the jet upstream of the inpingement is assumed to be

$$\frac{m_u}{m_u + m_d} = \lambda f\left(\frac{s_c}{t}\right) , \qquad [3]$$

a second expression for the mass flow, from the momentum balance, can be obtained:

$$\frac{m_u}{m_u + m_d} = \frac{1 - a\sin\varphi_c}{1 + b} \qquad [4]$$

where

$$a = \frac{\bar{u}}{\bar{u}_d}$$

$$b = \frac{\bar{u}_u}{\bar{u}_d}$$

m_u, m_d are the inward and outward mass flows respectively

$\bar{u}_u$, $\bar{u}_d$ are the average velocities of the inward and outward mass flows respectively.

Combining Equations [3] and [4] gives

$$\sin \varphi_c = \frac{1}{a}\left[1 - (1 + b)\ \lambda f\left(\frac{s_c}{t}\right)\right] . \qquad [5]$$

The impingement angle at the high side, $\varphi_{c,2}$, may be computed by using the same approximation as that used for balanced operation. The impingement angle at the low side, $\varphi_{c,1}$, may then be calculated from Equation [2]. It can be shown, however, that there is a critical tilt angle, α_{cr}, above which Equations [2] and [5] are no longer compatible; that is

$$\sin \varphi_{c,1} = \frac{1}{a_1}\left[1 - (1 + b_1)\ \lambda_1 f\left(\frac{s_{c,1}}{t}\right)\right] > \frac{H_1}{H_2} \sin \varphi_{c,2} + \left(1 - \frac{H_1}{H_2}\right) \sin \varphi_o \qquad [6]$$

where $a_1 = b_1 = 1$ for the equally split jet. The critical angle may be expressed, approximately, as follows:

$$\alpha_{cr} \doteq \sin^{-1}\left[\frac{H}{W}\left(\sin \varphi_{c,2} - \sin \varphi_s\right)\Big/\left(\sin \varphi_{c,2} + \sin \varphi_s - 2 \sin \varphi_o\right)\right] \qquad [7]$$

where $\sin \varphi_s$ is the impingement angle for the equally split jet. For $\alpha \geq \alpha_{cr}$, the jet at the low side becomes overfed.

Consider, first, the case $\alpha < \alpha_{cr}$. The flow pattern under the base plate is similar to that of an annular jet in hovering condition. The augmentation factor, including the effects of jet mixing and standing vortex, can be shown to be

$$A = \frac{L}{2J} = \cos \varphi_o + \frac{\sin \varphi_{c,2} - \sin \varphi_o}{H_2/W} + \lambda_2 f(\varphi_o, \frac{H}{t}) - \frac{1}{4}\left\{\frac{W_1}{t}\left[g\left(\frac{t}{H_1}, \gamma, n\right)\right]^2 + \frac{W_2}{t}\left[g\left(\frac{t}{H_2}, \gamma, n\right)\right]^2\right\} \qquad [8]$$

where

$$g(\frac{t}{H}, \gamma, n) = \frac{\bar{u}_{ave}}{U_e}$$

L	is the lift
n	is a number (=6 for large Reynolds number)
$\bar{u}_{ave}$	is the average induced velocity in the major vortex region
U_e	is the nozzle exit velocity
W	is the longitudinal size of the major standing vortex
γ	is a constant, depending on the local shearing stress.

The effect of the standing vortex on the augmentation factor is, in general, small; but it is the sole cause for inducing a moment due to the small tilt of a hovering ground effect machine. The induced moment about the center of the nozzle base plate, positive counterclockwise, may be expressed as

$$M_\alpha \doteq -\tfrac{1}{2}\rho U_e^2 W \left\{ w_1 \left(1 - \frac{w_1}{2W}\right)\left[g\left(\frac{t}{H_1}, \gamma, n\right)\right]^2 - w_2 \left(1 - \frac{w_2}{2W}\right)\left[g\left(\frac{t}{H_2}, \gamma, n\right)\right]^2 \right\} . \qquad [9]$$

Non-dimensionalizing by J × W, Equation [9] becomes

$$\overline{M}_\alpha \doteq -\tfrac{1}{2}\left(1 - \frac{w_1}{2W}\right)\left\{ \frac{w_1}{t}\left[g\left(\frac{t}{H_1}, \gamma, n\right)\right]^2 - \frac{w_2}{t}\left[g\left(\frac{t}{H_2}, \gamma, n\right)\right]^2 \frac{1 - \frac{w_2}{2W}}{1 - \frac{w_1}{2W}} \right\} . \qquad [10]$$

The longitudinal size of the standing vortex, w, is found to be directly proportional to the height of the machine according to the experimental studies of Poison-Quinton (6) and Nixon and Sweeny (7). Therefore, at very low heights, the induced moment may be shown, in general, to have a restoring or stabilizing effect; that is,

$$\frac{w_1}{t}\left[g\left(\frac{t}{H_1}, \gamma, n\right)\right]^2 < \frac{w_2}{t}\left[g\left(\frac{t}{H_2}, \gamma, n\right)\right]^2 \frac{1 - \frac{w_2}{2W}}{1 - \frac{w_1}{2W}}$$

since

$$g\left(\frac{t}{H_1}, \gamma, n\right) \doteq g\left(\frac{t}{H_2}, \gamma, n\right)$$

and

$$\frac{w_2}{w_1}\left(\frac{1 - \frac{w_2}{2W}}{1 - \frac{w_1}{2W}}\right) > 1.$$

At higher heights, due to the diffusing action of the jets,

$$g\left(\frac{t}{H_1}, \gamma, n\right) > g\left(\frac{t}{H_2}, \gamma, n\right)$$

and the induced moment may be found to be destabilizing. The tentative conclusion is qualitatively in agreement with the experimental observations of Helgesen and Rosenberg (8).

For large tilt angles, or $\alpha > \alpha_{cr}$, the jet flow field under the base plate is extremely complex because of the overfed flow condition on the low side. The cross flow, due to the viscous action of the fluid, may have dual effects on the static stability of the ground effect machine:

a) A stabilizing influence due to the friction effect.

b) A destabilizing effect due to diffusion.

For a machine very close to the ground, say $H < t$, the friction effect may be dominant and is stabilizing. The diffusion effect becomes important when the machine height is increased. In general, for practical heights, the diffusion effect always outweighs the friction effect. It may safely be concluded that, in practice, the overall effect of the cross flow is destabilizing.

It is very difficult to calculate the details of the cross flow field under ground effect machines; however, for the static stability analysis, which is essentially based on small disturbance theory, a simple and plausible approximation is afforded by assuming $\alpha < \alpha_{cr}$. The moments due to small disturbances, α, are readily given by Equation [10]. The stability derivative defined as the rate of change of moment with respect to α, $d\mathbf{M}_\alpha/d\alpha|\alpha \to 0$, may then be calculated.

A numerical example for the case $\alpha < \alpha_{cr}$, $\varphi_o = 0^o$ and $\frac{2W}{t} = 100$, has been made. The calculations are based on the simple assumption given in (1); that is, by assuming

$$w_1 = H_1 \quad , \quad w_2 = H_2$$

$$g\left(\frac{t}{H}, \gamma, n\right) = .66\,\{3\gamma\}^{\frac{n+1}{2n+3}} \qquad \text{for } \frac{H}{t} < 5.2$$

$$= .66\left\{1 + \left(\frac{2n}{n+2}\right)^{\frac{n}{n+1}}\left(\frac{5.2t}{H}\right)^{-\frac{1}{2(n+1)}}\left[\left(\frac{5.2t}{H}\right)^{-\frac{n+2}{2n}} - 1\right]^{\frac{n}{n+1}}\right\} \times$$

$$\left\{(3\gamma)\left(\frac{5.2t}{H}\right)\right\}^{\frac{n+1}{2n+3}} \qquad \text{for } \frac{H}{t} > 5.2$$

$$\gamma = .05 \quad , \quad n = 6$$

The augmentation factors, for various heights, were found to decrease with increasing tilt angles. These results are shown in Figure 2. The calculations of the induced moments, for various heights, are given in Figure 3; for $H/t > 5.2$, the induced moments were found to be always negative or destabilizing. The calculations of stability derivatives together with Lin's (9) thick and inviscid calculations assuming the moment coefficient, C, equal to 1/4, are given in Figure 4. It indicates that a much higher static stability boundary is predicted by the present calculations.

Although the above-mentioned illustration is based on the tilted ground effect machine model, the general conclusions are believed to be qualitatively true for all ground effect machines in unbalanced operations.

EFFECT OF FORWARD MOTION

Effects due to forward motion are responsible for important design and performance problems. The aerodynamic phenomena underlying the moving ground effect machine are extremely complex. The effects of forward speed are intimately connected with the aerodynamic form of the upper surface, intakes, and leading edge of the machine. The major concern here is to study the influence of forward speed on the behavior of the air jet curtain. At relatively low forward speeds, the air jet in the leading edge escapes upstream and the flow pattern in the air cushion is essentially the same as in the hovering condition. At high forward speeds, the air jet in the leading edge deflects inward before reaching the ground, and the flow underneath the machine resembles that of the jet-wing type. The flow regimes may be characterized by the thrust coefficient, C_μ, commonly used in boundary layer and flow control studies, defined as

$$C_\mu = \frac{q_m U_e}{\frac{1}{2}\rho U_o^2 S} \qquad [11]$$

where

q_m is the jet mass flow

S is the planform area of the nozzle base plate

U_o is the uniform forward speed

ρ is the air density.

At low forward speed, that is, in the ground cushion flow regime, the base pressure, p_b, is greater than the free stream total head, p_o, and acts to curve the jets outward. As the forward speed increases, the free stream total head becomes larger and larger. At a critical forward speed, $U_{o)cr}$,

$$p_b = p_o = p + \tfrac{1}{2}\rho U^2_{o)cr} \qquad [12]$$

where p is the free-stream static pressure. For a first-order approximation, the pressure inside the jet curtain is assumed to be uniform. The pressure difference across the jet in the leading edge is found to be

$$\Delta p_b = p_b - p \doteq \frac{J}{R} + 0\left(\frac{H}{2W}\right) \qquad [13]$$

where R is the radius of curvature of the jet curtain, and the critical thrust coefficient may be shown approximately to be

$$C_{\mu})_{cr} = \frac{J}{\frac{1}{2}\rho U_{o})_{cr}^{2}\, 2W} = \frac{R}{2W}\left|1 + 0\left(\frac{H}{2W}\right)\right|$$

$$\doteq \frac{R}{2W} \qquad \text{for } \frac{H}{2W} << 1. \qquad [14]$$

Below this critical value, the jet-wing type of flow evidently occurs. In the following, the case $C_\mu > C_{\mu})_{cr}$, that is, the ground cushion flow regime, is discussed in detail.

For easier conceptual and mathematical analysis, we shall superimpose upon the infinite stream and ground a uniform speed of the same magnitude as the machine forward speed, U_o; hence, the ground effect machine may be taken as stationary. The two-dimensional flow pattern, in this case, may be sketched as in Figure 5.

In the leading edge, the air jet in the leading edge escapes upstream after reaching the ground. Due to the action of the oncoming stream, the forward jet will separate upstream. The general flow pattern in the neighborhood of the leading edge is shown diagrammatically in Figure 6. The resultant flow is geometrically similar, if not physically, to the flow up a step. The forward jet and the machine base form the step. Separation occurs at the point B, somewhat upstream of the step. Beyond B, the external flow follows a streamline BC (which bounds a region of air very nearly at rest at constant pressure BCD) and then separates again behind the leading edge to form, roughly, another free streamline. The jet-type shear layer BC is probably assisted in remaining stable by the proximity of the boundary BDC. The external irrotational flow is indeterminate, taking different forms for various separation points, corresponding to different excess pressures in the "dead-air region". For each pressure assumed on the streamline BC, a different flow pattern then emerges. It is the position of separation, specified by the ratio ℓ/h (where ℓ is the distance from the step to separation and h is the step height), which will determine the actual shape of the streamline BC.

The free streamline theory needed to calculate the external flow (which is assumed to be stable) is straight-forward and is given by Lighthill (10). To a sufficient approximation, the excess pressure, Δp, in the dead-air region BCD may be shown to be

$$\Delta p \doteq \tfrac{1}{2}\rho U_o^2 \left(1 - e^{\frac{-\pi h}{\ell}}\right) . \qquad [15]$$

The values of $\frac{h}{\ell}$ in Equation [15], however, depend on the characteristics of the forward turbulent wall jet and the forward speed of the machine. For the present analysis, it is first assumed that the forward jet is fully turbulent and has the characteristics of the classical turbulent wall-jet (3), and the average mean jet velocity, $\overline{U}_j$, may be approximated as

$$\overline{U}_j \doteq \frac{.35U_e}{\sqrt{s_c/5.2t}} . \qquad [16]$$

The diffusing forward jet stream is brought to rest near the separation point due to the action of the oncoming free stream. For a first-order approximation, the values of ℓ may be obtained by equating

$$U_o = \overline{U}_j \doteq \frac{.35U_e}{\sqrt{(H+\ell)/5.2t}} \qquad [17]$$

or

$$\frac{\ell}{h} \doteq \frac{5.2t}{h}\left(.35\,\frac{U_e}{U_o}\right)^2 - \frac{H}{h} \,. \qquad [18]$$

Combining Equations [11], [15] and [18] gives

$$\frac{\Delta p}{\frac{1}{2}\rho U_o^{\,2}} = 1 - \exp\left(-\frac{\pi h}{.63WC_\mu - H}\right) . \qquad [19]$$

The pressure coefficient, $\Delta p/\frac{1}{2}\rho U_o^{\,2}$, is plotted against $1/C_\mu$ for different values of $\frac{H}{W}$ in Figure 7. In the calculations, the ground effect machine is assumed to have a very slender leading edge, that is, $h \doteq H$. It can be seen in Figure 7 that the pressure in the dead-air region increases rapidly with increasing $1/C_\mu$ or forward speed U_o. For simplicity, we shall assume that the upper surface of the machine is sufficiently smooth and no separation occurs on the trailing edge, so that the condition there is then approximately the same as that in the ambient region. Therefore, due to the pressure difference between the trailing and leading edges, there will be a difference in jet momentum in the direction of thrust, and its magnitude can be shown approximately to be

$$T = J_R - J_f \doteq R\Delta p = R\,(\tfrac{1}{2}\rho U_o^2)\left[1 - \exp\left(-\frac{\pi h}{.63WC_\mu - H}\right)\right] \qquad [20]$$

where

J_f is the front jet momentum per unit length = J

J_R is the rear jet momentum per unit length.

Non-dimensionalizing by J, Equation [20] becomes

$$\overline{T} = \frac{T}{J} \doteq \frac{R}{2WC_\mu}\left[1 - \exp\left(- \frac{\pi h}{.63WC_\mu - H}\right)\right] . \qquad [21]$$

Accordingly, a nose-down moment about the centerline of the machine, generated by the different front and rear jet reactions, may be shown to be

$$M_j = (J_R - J)W \doteq (R\Delta p)W = W\left(\tfrac{1}{2}\rho U_o^2\right) R\left[1 - \exp\left(- \frac{\pi h}{.63WC_\mu - H}\right)\right] . \qquad [22]$$

Non-dimensionalizing by J x W, Equation [22] becomes

$$\overline{M}_j = \frac{M_j}{JW} \doteq \frac{R}{2WC_\mu}\left[1 - \exp\left(- \frac{\pi h}{.63WC_\mu - H}\right)\right] . \qquad [23]$$

Inside the jet curtain, the general characteristics of the jet flow field are essentially the same as in the hovering condition. However, the strengths of the major standing vortex in the leading and trailing edges are modified somewhat by the motion of the ground and by the different edge jet momentums. On the front major eddy, the moving ground has a pulling effect and, as a result, the strength of the vorticity is increased there. On the rear major eddy, the strength of vorticity is, on the one hand, decreased due to the dragging effect of the moving ground and, on the other hand, increased due to the bigger rear jet momentum. In any event, the induced velocities in the leading and trailing edge vortices are, in general, different in magnitude; that is,

$$\bar{u}_{ave})_{\ell.e} \neq \bar{u}_{ave})_{t.e} \quad . \qquad [24]$$

Since the induced pressure loss, Δp_{vortex}, is proportional to the induced velocity, it is evident that

$$\Delta p_{vortex})_{\ell.e} \neq \Delta p_{vortex})_{t.e} \quad . \qquad [25]$$

As a consequence, a moment about the center of the machine, positive nose down, is induced and its magnitude may be shown approximately to be

$$M_{vortex} \doteq H \left[\Delta p_{vortex})_{\ell.e} - \Delta p_{vortex})_{t.e}\right]\left(1 - \frac{H}{2W}\right) W$$

$$\doteq \tfrac{1}{2}\rho\left[U_e^2 g_{\ell.e}^2 - U_{e,R}^2 g_{t.e}^2\right] H \left(1 - \frac{H}{2W}\right) W \qquad [26]$$

where

$$g_{\ell.e} = \frac{\bar{u}_{ave})_{\ell.e}}{U_e} = g_{\ell.e}\left(\frac{t}{H}, \gamma, n; \frac{U_o}{U_e}\right)$$

$$g_{t.e} = \frac{\bar{u}_{ave})_{t.e}}{U_{e,R}} = g_{t.e}\left(\frac{t}{H}, \gamma, n, \frac{U_o}{U_{e,R}}\right)$$

$U_{e,R}$ is the rear nozzle exit velocity.

Non-dimensionalizing by J × W, Equation [26] becomes

$$\overline{M}_{vortex} = \frac{M_{vortex}}{JW} \approx \tfrac{1}{2}\left(1 - \frac{H}{2W}\right)\frac{H}{t}\; g_{\ell.e}^{\,2}\left[1 - \left(\frac{g_{t.e}}{g_{\ell.e}}\right)^2 \frac{J_R}{J}\right] \qquad [27]$$

if the two nozzle exits are of equal thickness and divergence angles , where

$$\left.\begin{aligned} &\frac{g_{t.e}}{g_{\ell.e}} < 1 \qquad \text{(in general)} \\ &\frac{J_R}{J} = 1 + \frac{R}{2WC_\mu}\left[1 - \exp\left(-\frac{\pi h}{.63WC_\mu - H}\right)\right] \geq 1 \end{aligned}\right\} \qquad [28]$$

The direction of the induced moment due to the vortices depends on the parameter $(g_{t.e}/g_{\ell.e})^2 (J_R/J)$:

$$\left(\frac{g_{t.e}}{g_{\ell.e}}\right)^2\left(\frac{J_R}{J}\right) \begin{cases} < 1 & \text{nose down} \\ > 1 & \text{nose up} . \end{cases} \qquad [29]$$

The total non-dimensional induced moment due to forward motion on the jet flow fields under the machine base plate may be shown, by combining Equations [23] and [27], to be

$$\bar{M} = \bar{M}_j + \bar{M}_{vortex}$$

$$\doteq \left(\frac{J_R}{J} - 1\right) + \tfrac{1}{2}\left(1 - \frac{H}{2W}\right)\frac{H}{t}\, g_{\ell.e}^{2}\left[1 - \left(\frac{g_{t.e}}{g_{\ell.e}}\right)^{2}\frac{J_R}{J}\right] \quad [30]$$

It can be seen from Equation [28] that the term

$$\left(\frac{J_R}{J} - 1\right) >> \tfrac{1}{2}\left(1 - \frac{H}{2W}\right)\frac{H}{t}\, g_{\ell.e}^{2}\left[1 - \left(\frac{g_{t.e}^{2}}{g_{\ell.e}}\right)^{2}\frac{J_R}{J}\right] \quad [31]$$

since, in general, $g_{\ell.e}^{2} << 1$, and $\left(1 - \left(\frac{g_{t.e}}{g_{\ell.e}}\right)^{2}\frac{J_R}{J}\right) << 1$.

In view of Equations [27], [30] and [31], at low forward speeds, a nose-down moment is, in general, induced. The resultant moment due to the effect of the forward motion is, of course, very much dependent on the external flow conditions.

At high forward speeds, that is, $C_{\mu} < C_{\mu)cr}$, the air jet in the leading edge may deflect inward before reaching the ground. The jet flow under the base plate is then similar to the diffusive flow in the lee of a two-dimensional jet as studied by Rouse (11). Because of the formation of a standing eddy along the base plate, a reduction in base pressure results. In this condition the leading edge jet is preventing the useful pressure from acting on the base. For better efficiency the front jet should therefore be turned off and the flow is then identical to that of the jet-wing type. The problem of the jet flap within ground effect has been the subject of numerous experimental and theoretical investigations [see, for example, (12)] and is beyond the scope of the present investigations.

A typical numerical example for the case $C_\mu > C_{\mu})_{cr}$, $\varphi_o = 0^o$, and $\frac{2W}{t} = 100$, has been made. The calculations are based on the simple analysis given in (1); the values of R, $g_{\ell.e}$, $g_{t.e}$, γ, and n are then given by

$$R = \frac{H}{\sin \varphi_c}$$

$$g_{\ell.e} = .66\left[\varsigma\left(\frac{t}{H}, n\right) + \eta\left(\frac{t}{H}, \gamma, n, \frac{U_o}{U_e}\right)\right]^{\frac{1}{2n+3}} \times \left[(2\gamma)\ \frac{5.2t}{H}\right]^{\frac{n+1}{2n+3}}$$

$$g_{t.e} = .66\left[\varsigma\left(\frac{t}{H}, n\right) - \xi\left(\frac{t}{H}, \gamma, n, \frac{U_o}{U_{e,R}}\right)\right]^{\frac{1}{2n+3}} \times \left[(2\gamma)\ \frac{5.2t}{H}\right]^{\frac{n+1}{2n+3}}$$

$$\varsigma\left(\frac{t}{H}, n\right) = \left\{1 + \left(\frac{2n}{n+2}\right)^{\frac{n}{n+1}}\left(\frac{5.2t}{H}\right)^{-\frac{1}{2(n+1)}} \left[\left(\frac{5.2t}{H}\right)^{-\frac{n+2}{2n}} - 1\right]^{\frac{n}{n+1}}\right\}^{-(n+1)}$$

$$\eta\left(\frac{t}{H}, \gamma, n, \frac{U_o}{U_e}\right) = \left(\frac{U_o}{.66U_e}\right)^{2n+3} \left(\gamma \frac{5.2t}{H}\right)^{-(n+1)} =$$

$$\left[\frac{1}{.66\sqrt{\left(\frac{W}{t}\right) C_\mu}}\right]^{2n+3} \left[\gamma \frac{5.2t}{H}\right]^{-(n+1)}$$

$$\xi\left(\frac{t}{H}, \gamma, n, \frac{U_o}{U_{e,R}}\right) = \left(\frac{U_o}{.66U_{e,R}}\right)^{2n+3} \left(\gamma \frac{5.2t}{H}\right)^{-(n+1)} =$$

$$\left[\frac{1}{.66\sqrt{\left(\frac{W}{t}\right)\left(\frac{J_R}{J}\right) C_\mu}}\right]^{2n+3} \left[\gamma \frac{5.2t}{H}\right]^{-(n+1)}$$

$$\gamma = .05 , \quad n = 6.$$

The induced thrusts, for various heights, were found to increase with increasing $1/C_\mu$; these results are shown in Figure 8. It can be seen that a considerable amount of thrust may be obtained at relatively low forward speeds. The calculations of induced moments are given in Figure 9. The non-dimensional induced moments were found to be, in general, positive, that is, nose down and of the same magnitude as that of the non-dimensional induced thrust.

BIBLIOGRAPHY

1. "Viscous Effects on Balanced Jets in Ground Proximity", HYDRONAUTICS Technical Report 241-1, January, 1963, Issued Under U. S. Army Transportation Research Command Contract No. DA 44-177-TC-845.

2. Tulin, M. P., "On the Vertical Motions of Edge Jet Vehicles", Proc. of Symposium on Ground Effect Phenomena, Princeton University, October 1959.

3. Glauert, M. B., "The Wall Jet", J.F.M., Vol. 1, Part 6, December 1956.

4. Bakke, P., "An Experimental Investigation of a Wall Jet", J.F.M., Vol. 2, Part 5, November 1957.

5. Schwarz, W. H., and Cosart, W. P., "The Two-dimensional Turbulent Wall-Jet", J.F.M., Vol. 10, Part 4, June 1961.

6. Poisson-Quinton, P., "Study of a Current Plan for a Ground Effect Planform", Proc. of Symposium on Ground Effect Phenomena, Princeton University, October 1959.

7. Nixon, W. B., and Sweeny, T. E., "A Review of the Princeton Ground Effect Program", Proc. of Symposium on Ground Effect Phenomena, Princeton University, October 1959.

8. Helgesen, J. O., and Rosenberg, N. H., "An Experimental Investigation of the Stability Characteristics of a Hovering Air Cushion Vehicle", Grumman Research Department Memorandum RM-217, October 1962.

9. Lin, J. D., "Static Stability of Ground Effect Machine - Thick Jet Theory", HYDRONAUTICS, Incorporated Technical Report 011-2, June 1961.

10. Lighthill, M. J., "On Boundary Layers and Up-Stream Influences", Part I, Proc. Roy. Soc. of London, Ser. A, Vol. 217, p. 344, 1953.

11. Rouse, H., "Diffusion in the Lee of a Two-dimensional Jet", Ninth International Congress for Applied Mechanics, 1957.

12. Lachmann, G. D., "Boundary Layer and Flow Control", Vol I and II, Pergamon Press, 1961.

GEM

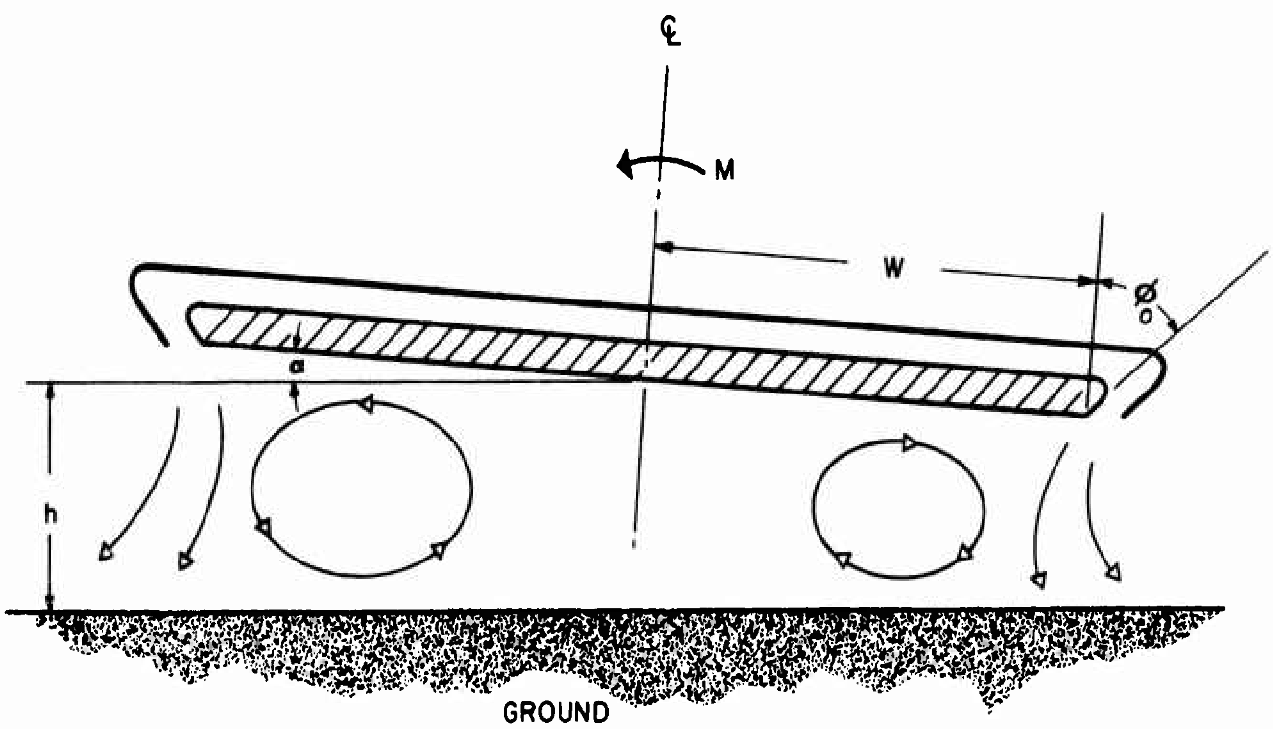

FIGURE 1 - TWO-DIMENSIONAL REPRESENTATION OF A SLIGHTLY TILTED GEM

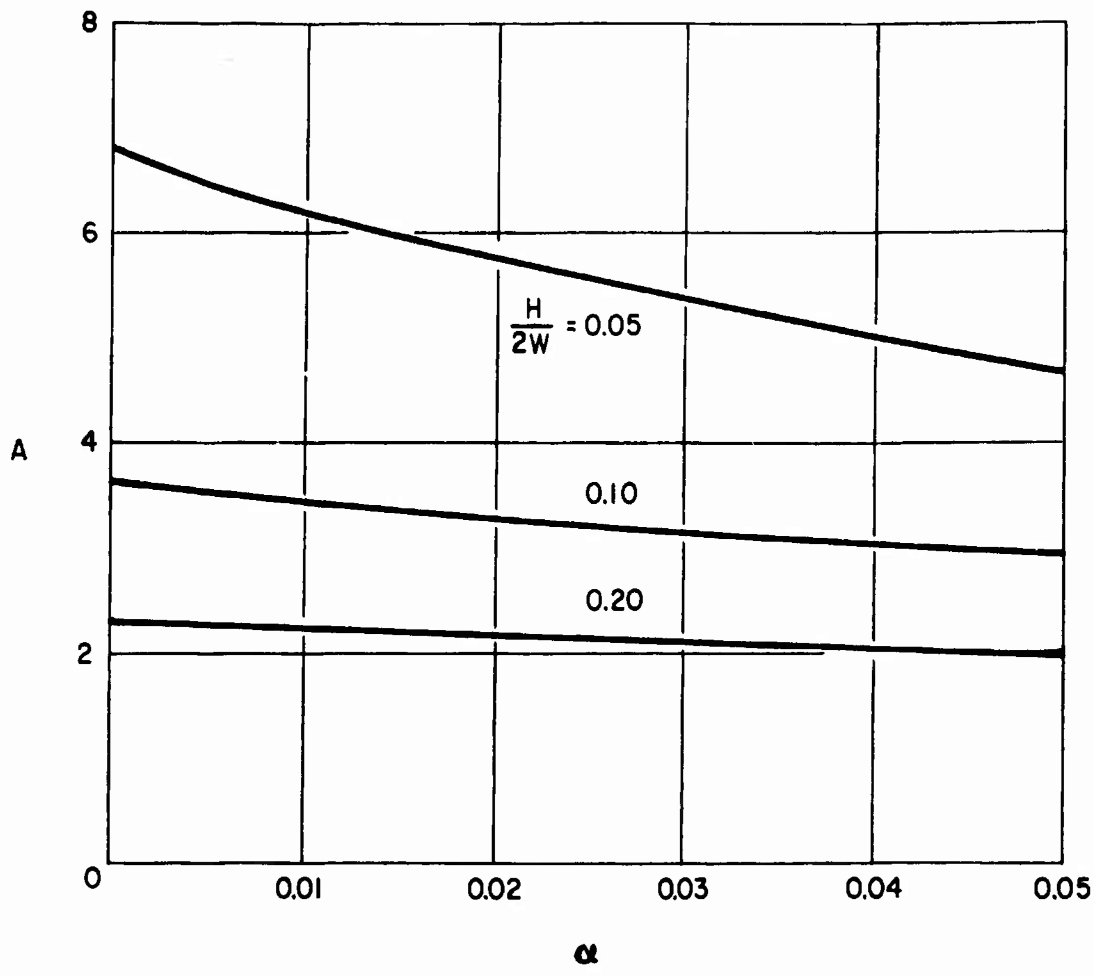

FIGURE 2 - EFFECT OF TILT ANGLE ON AUGMENTATION

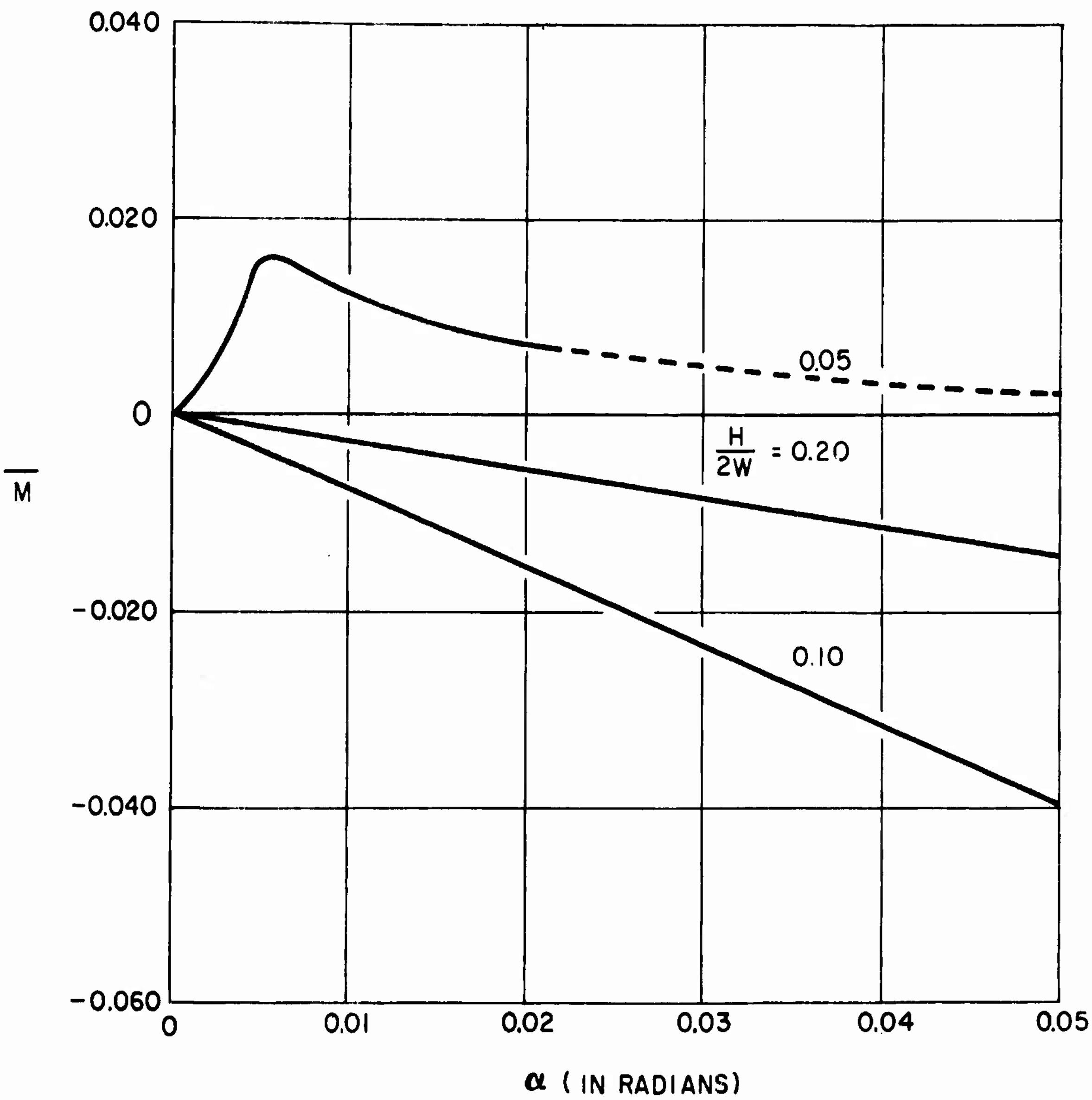

FIGURE 3 – EFFECT OF TILT ANGLE ON INDUCED MOMENT

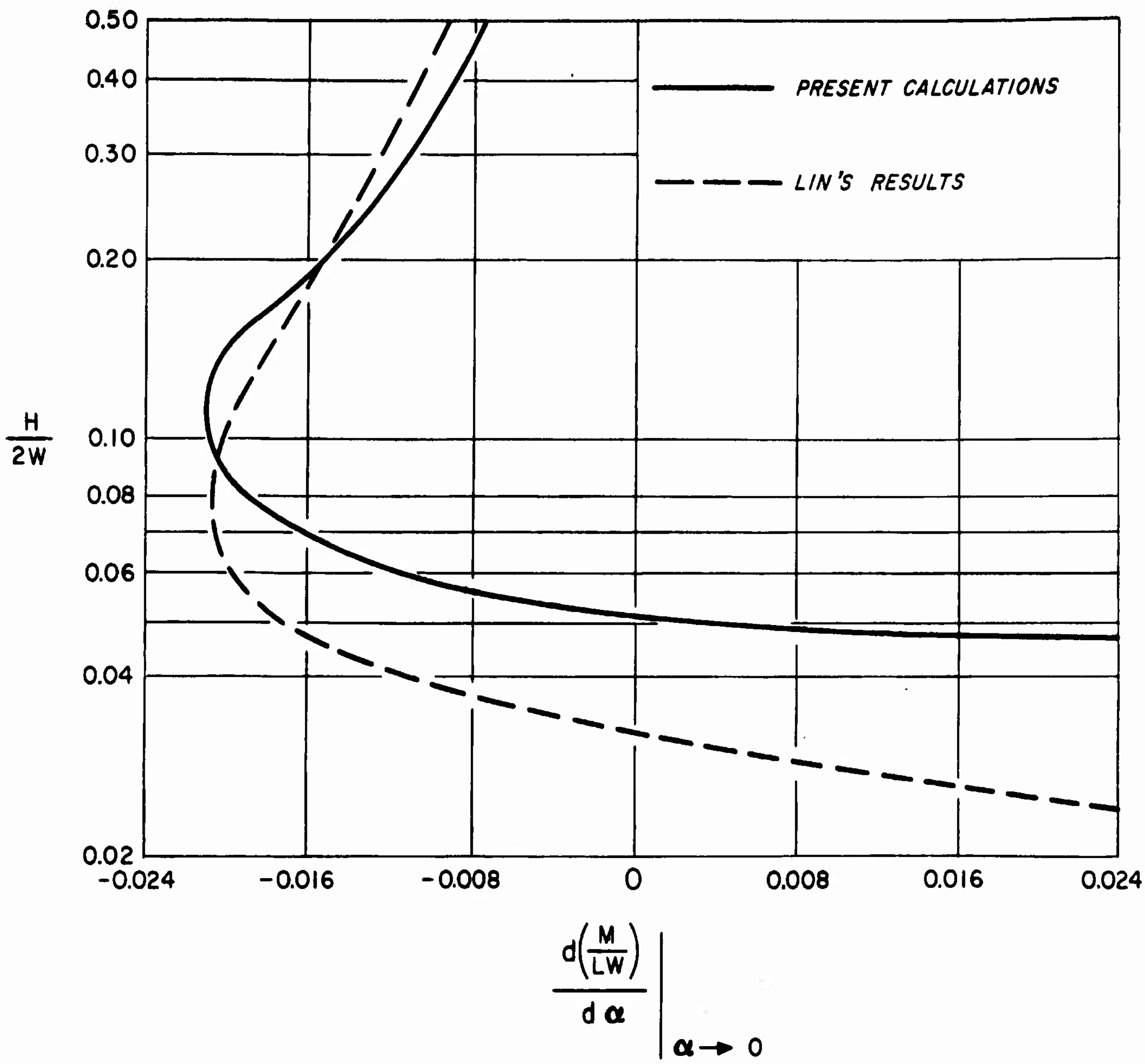

FIGURE 4 – STABILITY DERIVATIVES

GEM

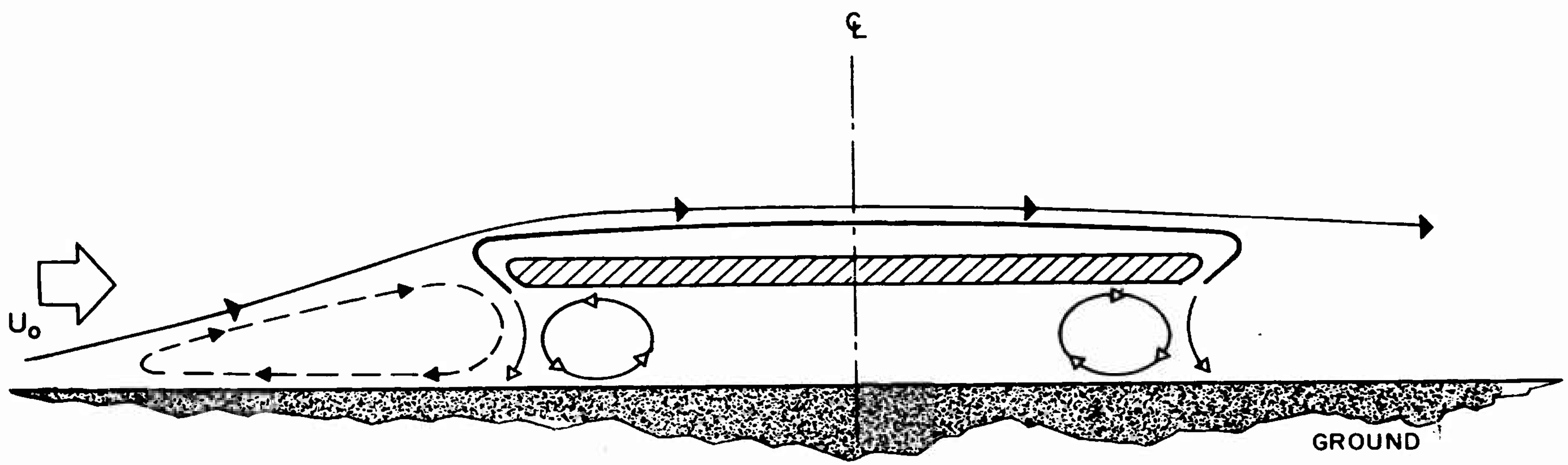

FIGURE 5 – TWO-DIMENSIONAL REPRESENTATION OF GEM IN FORWARD MOTION

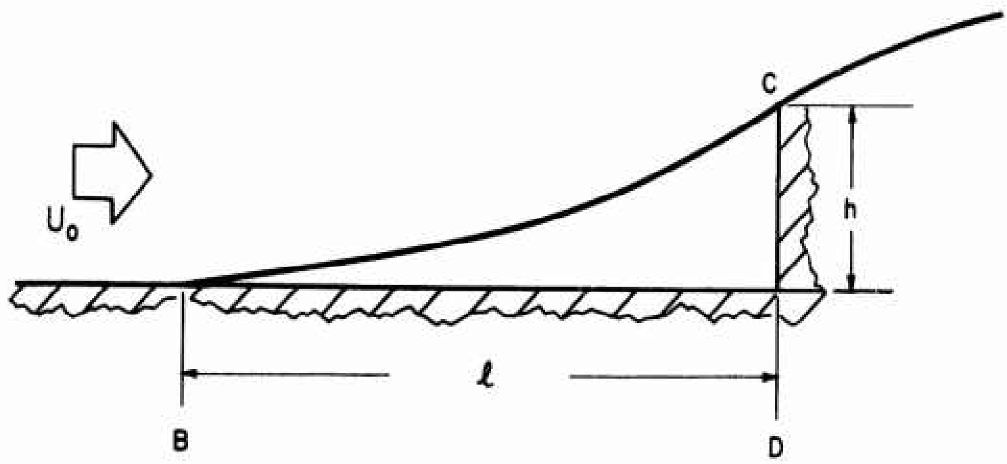

FIGURE 6 – DIAGRAM OF LOW-SPEED FLOW UP A STEP

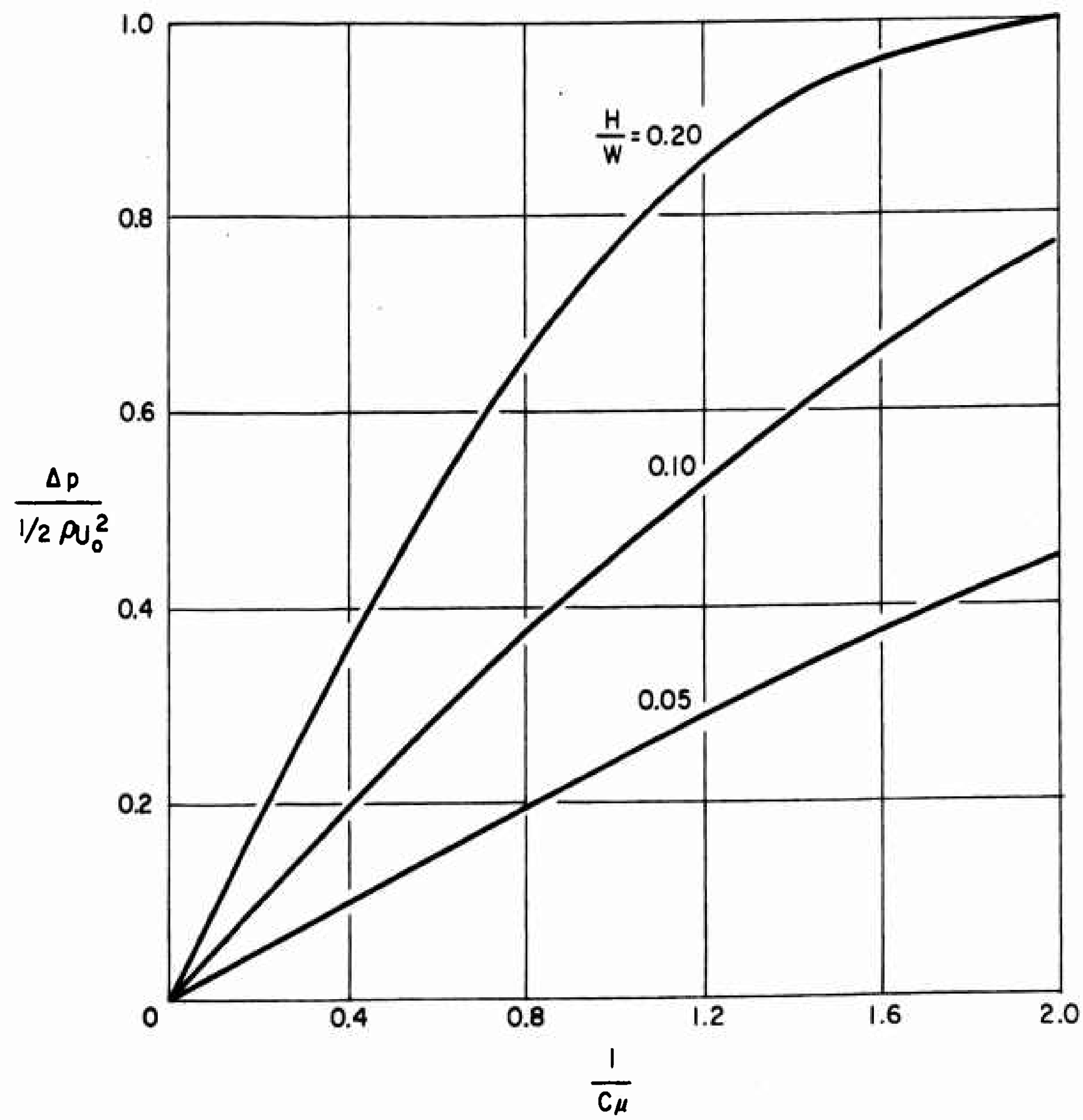

FIGURE 7 - EFFECT OF FORWARD SPEED ON PRESSURE COEFFICIENT IN DEAD - AIR REGION

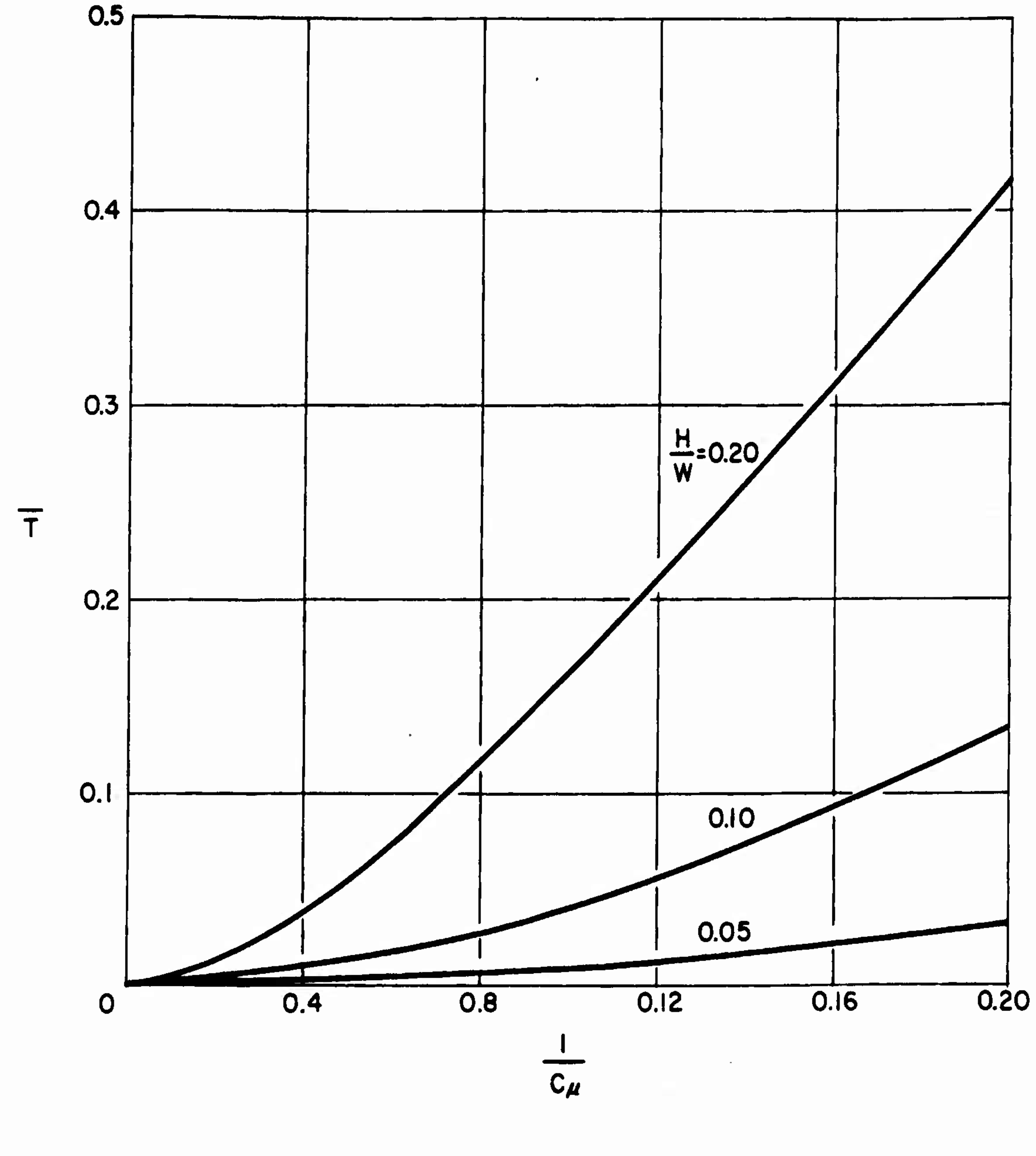

FIGURE 8 - EFFECT OF FORWARD SPEED ON INDUCED THRUST

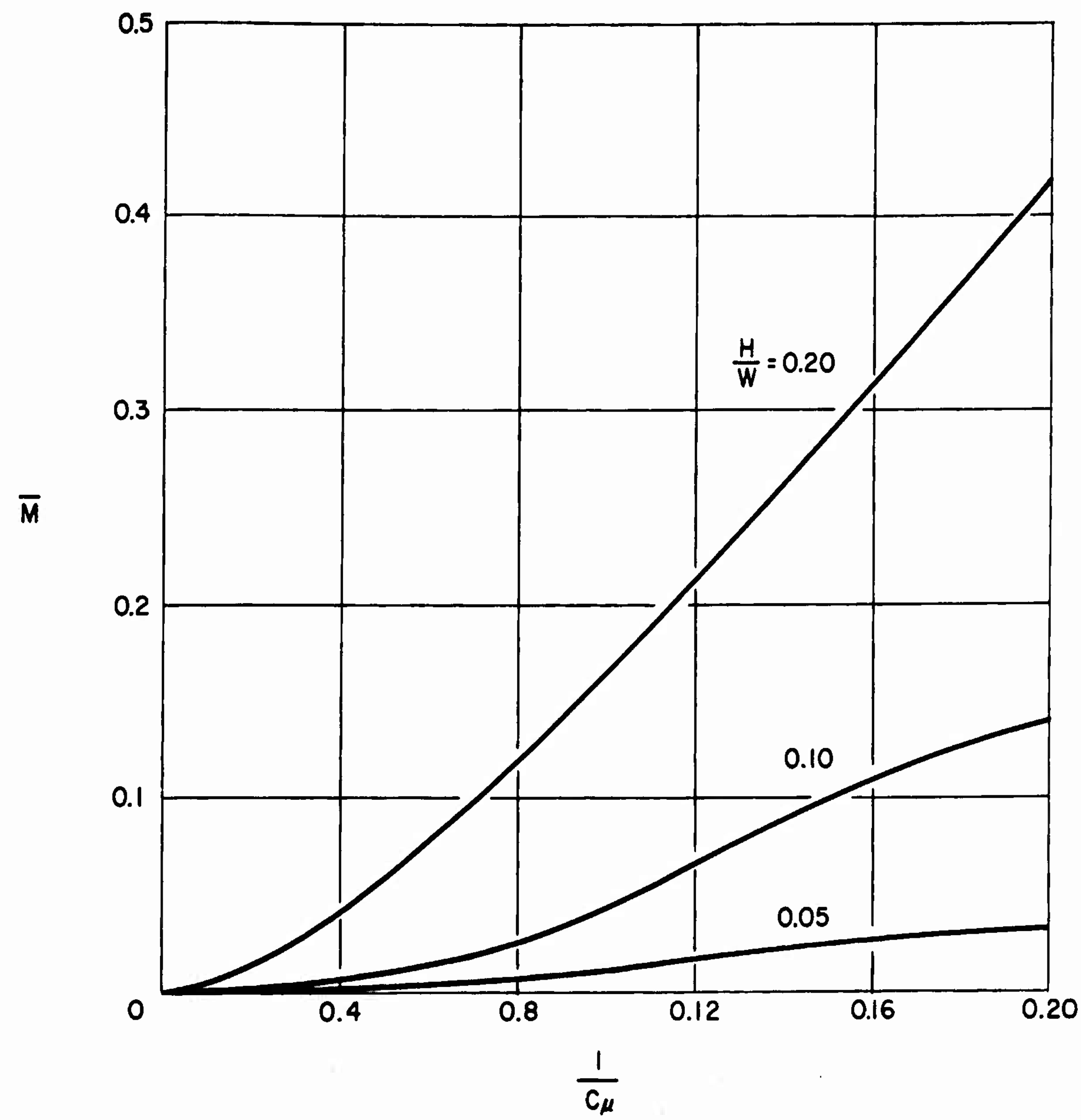

FIGURE 9 - EFFECT OF FORWARD SPEED ON INDUCED MOMENT

DISTRIBUTION

Army War College	1
Aviation Test Office	1
U. S. Army Polar Research and Development Center	1
Deputy Chief of Staff for Logistics, D/A	1
The Research Analysis Corporation	1
Army Research Office, Durham	2
Office of Chief of R&D, D/A	2
Naval Air Test Center	1
Army Research Office, D/A	1
Deputy Chief of Staff for Military Operations, D/A	1
U. S. Army Engineer Research and Development Laboratories	2
U. S. Army Tank-Automotive Center	2
The Ordnance Board	1
U. S. Army Combat Developments Command Transportation Agency	1
U. S. Army Aviation and Surface Materiel Command	2
U. S. Army Transportation Research Command	66
U. S. Army Transportation School	4
U. S. Army Airborne, Electronics and Special Warfare Board	1
U. S. Army Research and Development Group (Europe)	2
Chief of Naval Operations	1
Bureau of Naval Weapons	2
Bureau of Supplies and Accounts, D/N	1
U. S. Naval Supply Research and Development Facility	1
U. S. Naval Postgraduate School	1
Bureau of Ships, D/N	1
U. S. Naval Ordnance Test Station	1
David Taylor Model Basin	1
Marine Corps Schools	2
U. S. Army Standardization Group, Canada	1
Canadian Army Liaison Officer, U. S. Army Transportation School	3
British Army Staff, British Embassy	4
U. S. Army Standardization Group, U. K.	1
NASA-LRC, Langley Station	2
Ames Research Center	2
NASA Representative, Scientific and Technical Information Facility	1

U. S. Government Printing Office	1
Defense Documentation Center	10
U. S. Army Medical Research and Development Command	1
Human Resources Research Office	2
U. S. Strike Command	1
U. S. Army Mobility Command	3
U. S. Army Materiel Command	6
U. S. Army Human Engineering Laboratories	1
Office of the Asst. Secretary of Defense for R&E	1
U. S. Maritime Administration	1

HYDRONAUTICS, Incorporated, Laurel, Md., VISCOUS AND FORWARD SPEED EFFECTS ON UNBALANCED JETS IN GROUND PROXIMITY - C. C. Hsu, TRECOM Technical Report 63-60, October 1963, 33 pp. (Contract DA 44-177-TC-845) USATRECOM Task 1D021701A04804.

Unclassified Report

A theoretical investigation of two-dimensional ground effect machines in unbalanced opera-

1. Air Jet Flow Fields in Ground Proximity, Theory
2. C. C. Hsu
3. Contract DA 44-177-TC-845

HYDRONAUTICS, Incorporated, Laurel, Md., VISCOUS AND FORWARD SPEED EFFECTS ON UNBALANCED JETS IN GROUND PROXIMITY - C. C. Hsu, TRECOM Technical Report 63-60, October 1963, 33 pp. (Contract DA 44-177-TC-845) USATRECOM Task 1D021701A04804.

Unclassified Report

A theoretical investigation of two-dimensional ground effect machines in unbalanced opera-

1. Air Jet Flow Fields in Ground Proximity, Theory
2. C. C. Hsu
3. Contract DA 44-177-TC-845

HYDRONAUTICS, Incorporated, Laurel, Md., VISCOUS AND FORWARD SPEED EFFECTS ON UNBALANCED JETS IN GROUND PROXIMITY - C. C. Hsu, TRECOM Technical Report 63-60, October 1963, 33 pp. (Contract DA 44-177-TC-845) USATRECOM Task 1D021701A04804.

Unclassified Report

A theoretical investigation of two-dimensional ground effect machines in unbalanced opera-

1. Air Jet Flow Fields in Ground Proximity, Theory
2. C. C. Hsu
3. Contract DA 44-177-TC-845

HYDRONAUTICS, Incorporated, Laurel, Md., VISCOUS AND FORWARD SPEED EFFECTS ON UNBALANCED JETS IN GROUND PROXIMITY - C. C. Hsu, TRECOM Technical Report 63-60, October 1963, 33 pp. (Contract DA 44-177-TC-845) USATRECOM Task 1D021701A04804.

Unclassified Report

A theoretical investigation of two-dimensional ground effect machines in unbalanced opera-

1. Air Jet Flow Fields in Ground Proximity, Theory
2. C. C. Hsu
3. Contract DA 44-177-TC-845

tion and forward motion is presented. In unbalanced operation, the formation of two counter-rotating vortices is the sole cause for inducing static instability for small disturbances. The occurence of cross flow for large disturbances is, in general, destabilizing. In forward motion, two distinct flow regimes, i.e., ground cushion flow and jet-wing type of flow, may appear. Considerable amount of thrust and nose-down moment may be induced in the ground cushion flow regime. Quantitative results pertaining to the above effects are presented.

tion and forward motion is presented. In unbalanced operation, the formation of two counter-rotating vortices is the sole cause for inducing static instability for small disturbances. The occurence of cross flow for large disturbances is, in general, destabilizing. In forward motion, two distinct flow regimes, i.e., ground cushion flow and jet-wing type of flow, may appear. Considerable amount of thrust and nose-down moment may be induced in the ground cushion flow regime. Quantitative results pertaining to the above effects are presented.

tion and forward motion is presented. In unbalanced operation, the formation of two counter-rotating vortices is the sole cause for inducing static instability for small disturbances. The occurence of cross flow for large disturbances is, in general, destabilizing. In forward motion, two distinct flow regimes, i.e., ground cushion flow and jet-wing type of flow, may appear. Considerable amount of thrust and nose-down moment may be induced in the ground cushion flow regime. Quantitative results pertaining to the above effects are presented.

tion and forward motion is presented. In unbalanced operation, the formation of two counter-rotating vortices is the sole cause for inducing static instability for small disturbances. The occurence of cross flow for large disturbances is, in general, destabilizing. In forward motion, two distinct flow regimes, i.e., ground cushion flow and jet-wing type of flow, may appear. Considerable amount of thrust and nose-down moment may be induced in the ground cushion flow regime. Quantitative results pertaining to the above effects are presented.

HYDRONAUTICS, Incorporated, Laurel, Md., VISCOUS AND FORWARD SPEED EFFECTS ON UNBALANCED JETS IN GROUND PROXIMITY - C. C. Hsu, TRECOM Technical Report 63-60, October 1963, 33 pp. (Contract DA 44-177-TC-845) USATRECOM Task 1D021701A04804.

Unclassified Report

A theoretical investigation of two-dimensional ground effect machines in unbalanced opera-

1. Air Jet Flow Fields in Ground Proximity, Theory
2. C. C. Hsu
3. Contract DA 44-177-TC-845

HYDRONAUTICS, Incorporated, Laurel, Md., VISCOUS AND FORWARD SPEED EFFECTS ON UNBALANCED JETS IN GROUND PROXIMITY - C. C. Hsu, TRECOM Technical Report 63-60, October 1963, 33 pp. (Contract DA 44-177-TC-845) USATRECOM Task 1D021701A04804.

Unclassified Report

A theoretical investigation of two-dimensional ground effect machines in unbalanced opera-

1. Air Jet Flow Fields in Ground Proximity, Theory
2. C. C. Hsu
3. Contract DA 44-177-TC-845

HYDRONAUTICS, Incorporated, Laurel, Md., VISCOUS AND FORWARD SPEED EFFECTS ON UNBALANCED JETS IN GROUND PROXIMITY - C. C. Hsu, TRECOM Technical Report 63-60, October 1963, 33 pp. (Contract DA 44-177-TC-845) USATRECOM Task 1D021701A04804.

Unclassified Report

A theoretical investigation of two-dimensional ground effect machines in unbalanced opera-

1. Air Jet Flow Fields in Ground Proximity, Theory
2. C. C. Hsu
3. Contract DA 44-177-TC-845

HYDRONAUTICS, Incorporated, Laurel, Md., VISCOUS AND FORWARD SPEED EFFECTS ON UNBALANCED JETS IN GROUND PROXIMITY - C. C. Hsu, TRECOM Technical Report 63-60, October 1963, 33 pp. (Contract DA 44-177-TC-845) USATRECOM Task 1D021701A04804.

Unclassified Report

A theoretical investigation of two-dimensional ground effect machines in unbalanced opera-

1. Air Jet Flow Fields in Ground Proximity, Theory
2. C. C. Hsu
3. Contract DA 44-177-TC-845

tion and forward motion is presented. In unbalanced operation, the formation of two counter-rotating vortices is the sole cause for inducing static instability for small disturbances. The occurence of cross flow for large disturbances is, in general, destabilizing. In forward motion, two distinct flow regimes, i.e., ground cushion flow and jet-wing type of flow, may appear. Considerable amount of thrust and nose-down moment may be induced in the ground cushion flow regime. Quantitative results pertaining to the above effects are presented.

tion and forward motion is presented. In unbalanced operation, the formation of two counter-rotating vortices is the sole cause for inducing static instability for small disturbances. The occurence of cross flow for large disturbances is, in general, destabilizing. In forward motion, two distinct flow regimes, i.e., ground cushion flow and jet-wing type of flow, may appear. Considerable amount of thrust and nose-down moment may be induced in the ground cushion flow regime. Quantitative results pertaining to the above effects are presented.

tion and forward motion is presented. In unbalanced operation, the formation of two counter-rotating vortices is the sole cause for inducing static instability for small disturbances. The occurence of cross flow for large disturbances is, in general, destabilizing. In forward motion, two distinct flow regimes, i.e., ground cushion flow and jet-wing type of flow, may appear. Considerable amount of thrust and nose-down moment may be induced in the ground cushion flow regime. Quantitative results pertaining to the above effects are presented.

tion and forward motion is presented. In unbalanced operation, the formation of two counter-rotating vortices is the sole cause for inducing static instability for small disturbances. The occurence of cross flow for large disturbances is, in general, destabilizing. In forward motion, two distinct flow regimes, i.e., ground cushion flow and jet-wing type of flow, may appear. Considerable amount of thrust and nose-down moment may be induced in the ground cushion flow regime. Quantitative results pertaining to the above effects are presented.

UNCLASSIFIED

UNCLASSIFIED